Formation and Characterization of the Photochemically Interconvertible Side-On and End-On Bonded Dioxygen−Iron Dioxide Complexes in Solid Argon

Yu Gong,[†] Mingfei Zhou,*[,†] and Lester Andrews[‡]

Department of Chemistry, Shanghai Key Laboratory of Molecular Catalysts and Innovative Materials, Advanced Materials Laboratory, Fudan University, Shanghai 200433, P. R. China, and Department of Chemistry, University of Virginia, Charlottesville, Virginia 22901

Received: August 15, 2007; In Final Form: September 13, 2007

Two interconvertible iron dioxide−dioxygen complexes were prepared and characterized by matrix isolation infrared absorption spectroscopy as well as theoretical calculations. Iron atoms react with O_2 to form the inserted FeO_2 molecule in solid argon only upon UV−visible light irradiation. Annealing allows the dioxygen molecules to diffuse and to react with FeO_2 and form the side-on and end-on bonded dioxygen−iron dioxide complexes, $(\eta^2\text{-}O_2)FeO_2$ and $(\eta^1\text{-}O_2)FeO_2$. The side-on bonded structure is a peroxide complex having a singlet ground state with a nonplanar C_{2v} symmetry. The end-on bonded isomer is characterized to be a superoxide complex with a planar $^3A''$ ground state. These two isomers are photoreversible, that is, near-infrared light ($\lambda > 850$ nm) induces the conversion of the side-on bonded $(\eta^2\text{-}O_2)FeO_2$ complex to the end-on bonded $(\eta^1\text{-}O_2)FeO_2$ isomer and vice versa with red light irradiation ($\lambda > 600$ nm).

Introduction

Oxidation of iron is an important subject in chemistry. Great efforts have been made on the preparation and characterization of iron oxides and dioxygen complexes in understanding the structure, bonding, and reactivity of them, which are regarded as important intermediates in processes such as material corrosion and biochemical oxidation.[1] The products of simple reactions between iron atoms and molecular oxygen have been intensively studied both experimentally and theoretically.[2−18] The cyclic $Fe(O_2)$, linear FeOO, and inserted OFeO molecules, as well as higher oxide complex species such as FeO_4, were all reported to be reaction products. In an early matrix isolation infrared spectroscopic study on the reaction of thermally evaporated iron atoms with dioxygen, absorptions at 945.9 and 517.1 cm^{-1} were assigned to vibrations of the cyclic $Fe(O_2)$ molecule in solid argon.[2] In the next work, three FeO_2 isomers were proposed to be formed from the reactions of hollow-cathode sputtered iron atoms with dioxygen in argon.[3] A band at 956 cm^{-1} was assigned to the O−O stretching mode of the cyclic $Fe(O_2)$ structure, while the bands at 969 and 946 cm^{-1} were attributed to the linear and bent OFeO isomers. In the photooxidation of matrix isolated iron pentacarbonyl in the presence of oxygen, a 956 cm^{-1} absorption was also assigned to the cyclic $Fe(O_2)$ molecule, but a 945 cm^{-1} absorption was attributed to FeO_3 instead of OFeO.[4] More recent investigations employed the reactions of laser ablated iron atoms with dioxygen,[5,6] and the absorption at 956.0 cm^{-1} was retained for cyclic $Fe(O_2)$, but absorptions at 945.8 and 797.1 cm^{-1} were assigned to the antisymmetric and symmetric stretching modes of the inserted FeO_2 molecule, while an absorption at 1204.5 cm^{-1} was characterized as the O−O stretching mode of an FeOO isomer.[6]

In contrast to the matrix isolation studies, gas phase investigations indicate that ground state iron atoms are unreactive toward dioxygen at room temperature.[7,8] Anion photoelectron spectroscopic investigation on FeO_2^- indicates that only the inserted FeO_2 neutral structure was observed.[9,10] Apparently, the reaction mechanism and the product identifications are still open to question. Hence, the reaction of iron atoms and dioxygen are reinvestigated using matrix isolation infrared absorption spectroscopy with lower laser energies and emission plume intensities. We will show that iron atoms react with dioxygen to form the inserted FeO_2 molecule only under UV−visible light excitation and that isolated cyclic $Fe(O_2)$ and FeOO species are not formed. The previous assignments to FeOO (1204.5 cm^{-1}) and cyclic $Fe(O_2)$ (956.0 cm^{-1}) in solid argon are incorrect.[3−6] These absorptions are reassigned to the end-on and side-on bonded dioxygen−iron dioxide complexes formed by the reactions of FeO_2 with dioxygen in the matrix.

Experimental and Computational Methods

The experimental setup for pulsed laser evaporation and matrix isolation infrared spectroscopic investigation has been described in detail previously.[19] Briefly, the 1064 nm fundamental of a Nd:YAG laser (Continuum, Minilite II, 10 Hz repetition rate and 6 ns pulse width) was focused onto a rotating iron metal target through a hole in a CsI window cooled normally to 6 K by means of a closed-cycle helium refrigerator (ARS, 202N). The laser-evaporated metal atoms were co-deposited with dioxygen/argon mixtures onto the CsI window. In general, matrix samples were deposited for 1 h at a rate of approximately 4 mmol/h. The O_2/Ar mixtures were prepared in a stainless steel vacuum line using standard manometric technique. Isotopic $^{18}O_2$ (ISOTEC, 99%) was used without further purification. The infrared absorption spectra of the resulting samples were recorded on a Bruker IFS 66V spectrometer at 0.5 cm^{-1} resolution between 4000 and 450 cm^{-1} using a liquid nitrogen cooled HgCdTe (MCT) detector. Samples were annealed to different temperatures and cooled back to 6

* To whom correspondence should be addressed. E-mail: mfzhou@fudan.edu.cn.
† Fudan University.
‡ University of Virginia.

10.1021/jp0765805 CCC: $37.00
Published on Web 11/07/2007

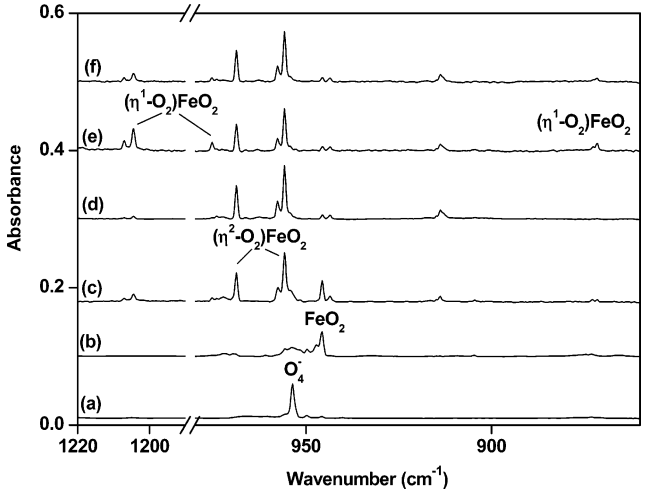

Figure 1. Infrared spectra in the 1220−1190 and 980−860 cm^{-1} regions from co-deposition of laser-evaporated Fe atoms with 1.0% O_2 in argon: (a) 1 h of sample deposition at 6 K, (b) after 15 min of broad band irradiation ($250 < \lambda < 580$ nm), (c) after annealing to 25 K, (d) after annealing to 35 K, (e) after 15 min of $\lambda > 850$ nm irradiation, and (f) after 15 min of $\lambda > 600$ nm irradiation. Spectra c, e, and f were taken with six scans and others with 200 scans.

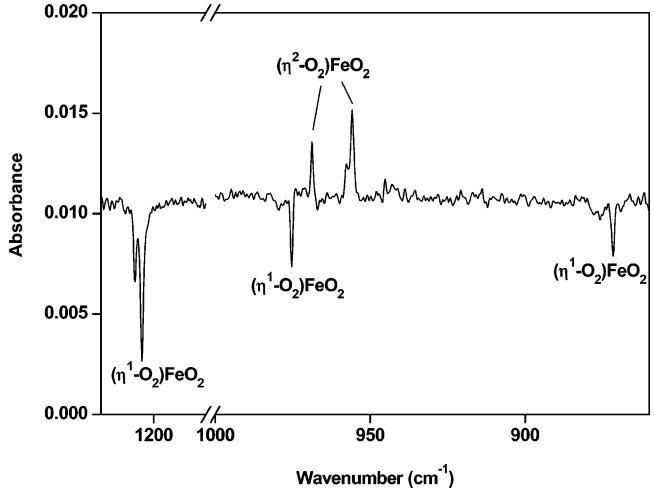

Figure 2. Difference IR spectrum in the 1220−1180 and 1000−860 cm^{-1} regions from co-deposition of laser-evaporated iron atoms with 1.0% O_2 in argon (spectrum taken 15 min after 25 K annealing minus spectrum taken right after 25 K annealing).

K for spectral acquisition. Selected samples were subjected to broad band irradiation using a tungsten lamp or a high-pressure mercury arc lamp with glass filters.

Quantum chemical calculations were performed using the Gaussian 03 program.[20] The three-parameter hybrid functional according to Becke with additional correlation corrections due to Lee, Yang, and Parr (B3LYP)[21,22] was utilized. The 6-311+G-(d) basis set was used for the O atom, and the all-electron basis set of Wachters−Hay as modified by Gaussian was used for the Fe atom.[23] The geometries were fully optimized; the harmonic vibrational frequencies were calculated, and zero-point vibrational energies (ZPVE) were derived. The single-point energies of all the structures optimized at the B3LYP level of theory were calculated using the CCSD(T) method with the same basis set.

Results and Discussions

Infrared Spectra. The experiments were performed using relatively low laser energy to minimize the formation of multinuclear species. The infrared spectra in selected regions from co-deposition of laser-evaporated iron atoms with 1.0% O_2 in argon using approximately 7 mJ/pulse laser energy are shown in Figure 1. After 1 h of sample deposition at 6 K, only the O_4^- absorption at 953.8 cm^{-1} was observed (Figure 1, trace a).[24] Broad band irradiation with the output of a high-pressure mercury arc lamp ($250 < \lambda < 580$ nm) destroyed the O_4^- absorption and produced two absorptions at 945.8 and 797.1 cm^{-1}, which were previously assigned to the antisymmetric and symmetric stretching modes of the inserted FeO_2 molecule (Figure 1, trace b).[6] When the sample was annealed to 25 K (Figure 1, trace c), the FeO_2 absorptions decreased with the formation of new absorptions at 1204.5, 1094.7, 975.3, 968.8, 955.8, 871.6, 558.1, and 548.3 cm^{-1}. These absorptions can be classified into two groups based on their annealing and photochemical behaviors. The IR intensities of the 1204.5, 975.3, and 871.6 cm^{-1} absorptions markedly increased when the sample was subjected to near-infrared irradiation using a tungsten lamp with a $\lambda > 850$ nm long wavelength pass filter, during which the IR intensities of another group of absorptions at 1094.7, 968.8, 955.8, 558.1, and 548.3 cm^{-1} decreased (Figure 1, trace e). In contrast, the 1094.7, 968.8, 955.8, 558.1, and 548.3 cm^{-1} absorptions increased at the expense of the 1204.5, 975.3, and 871.6 cm^{-1} absorptions when the sample was irradiated by the output of the tungsten lamp with a $\lambda > 600$ nm long wavelength pass filter (Figure 1, trace f). It is interesting to note that the IR intensities of the 1204.5, 975.3, and 871.6 cm^{-1} absorptions decreased, while the 1094.7, 968.8, 955.8, 558.1, and 548.3 cm^{-1} absorptions increased with increasing the sample scan times, during which the sample was irradiated by the light emitted from the source, as clearly demonstrated in Figure 2. However, the IR intensities of these product absorptions do not change significantly if the sample was kept in the dark. It should be pointed out that the ArFeO absorptions (873.1 cm^{-1}, this absorption was previously assigned to FeO, but recent investigation in this group indicates that it should be regarded as ArFeO isolated in solid argon)[25] were barely observed with low ablation laser energy.

In another experiment with the same laser energy and O_2 concentration as those in the experiment used for Figure 1, the sample was subjected to annealing directly after deposition without UV−visible irradiation. The 945.8 and 797.1 cm^{-1} absorptions previously assigned to FeO_2 were not formed,[6] and it is noteworthy that neither the 1204.5, 975.3, and 871.6 cm^{-1} absorptions nor the 1094.7, 968.8, 955.8, 558.1, and 548.3 cm^{-1} absorptions were produced on sample annealing.

Experiments were repeated using isotopic substituted $^{18}O_2$, $^{16}O_2 + {}^{18}O_2$ (1:1), and $^{16}O_2 + {}^{16}O^{18}O + {}^{18}O_2$ (1:2:1) mixtures. The spectra in selected regions with different isotopic samples are shown in Figures 3 and 4, respectively. The band positions of the new product absorptions are summarized in Table 1.

$(\eta^1\text{-}O_2)FeO_2$. The 1204.5 cm^{-1} absorption was previously assigned to the O−O stretching mode of a FeOO complex.[6] The isotopic shift and splittings observed in the present experiments indicate that this absorption is due to an O−O stretching mode with two slightly inequivalent O atoms, which are exactly the same as those previously reported.[6] However, the present experimental observations do not support the isolated FeOO assignment but favor this functional group in a larger complex. As has been mentioned above, the 1204.5 cm^{-1} absorption was only observed on annealing. Its IR intensity depends strongly on the inserted FeO_2 absorptions. It was not formed on annealing if the FeO_2 molecules were not presented in the matrix sample. As shown in Figures 1 and 2, two other

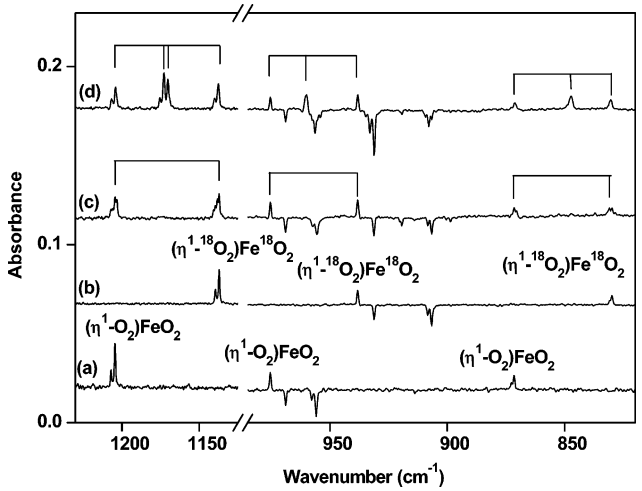

Figure 3. Difference IR spectra in the 1230−1125 and 985−820 cm^{-1} regions (spectra were taken after 35 K annealing followed by 15 min of $\lambda > 850$ nm irradiation) with different isotopic samples. Bands of (η^1-O$_2$)FeO$_2$ are pointing upward, and bands of (η^2-O$_2$)FeO$_2$ are pointing downward: (a) 1.0% $^{16}O_2$, (b) 1.0% $^{18}O_2$, (c) 0.5% $^{16}O_2$ + 0.5% $^{18}O_2$, and (d) 0.25% $^{16}O_2$ + 0.5% $^{16}O^{18}O$ + 0.25% $^{18}O_2$.

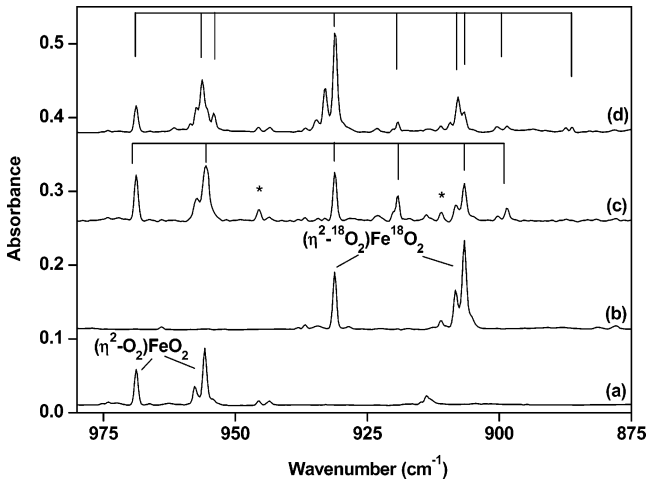

Figure 4. Infrared spectra in the 980−875 cm^{-1} region from co-deposition of laser-evaporated iron atoms with isotopic labeled O_2 in excess argon. Spectra were taken after 15 min of broad band irradiation followed by 35 K annealing: (a) 1.0% $^{16}O_2$, (b) 1.0% $^{18}O_2$, (c) 0.5% $^{16}O_2$ + 0.5%$^{18}O_2$, and (d) 0.25% $^{16}O_2$ + 0.5% $^{16}O^{18}O$ + 0.25% $^{18}O_2$. The asterisks denote FeO_2 and $Fe^{18}O_2$ absorptions.

absorptions at 975.3 and 871.6 cm^{-1} were observed to exhibit identical behavior upon annealing and irradiation along with the 1204.5 cm^{-1} absorption, which indicates that these three absorptions belong to different vibrational modes of the same species. The 975.3 and 871.6 cm^{-1} absorptions shifted to 938.1 and 929.9 cm^{-1} with $^{18}O_2$. The resulting $^{16}O/^{18}O$ isotopic frequency ratios of 1.0397 and 1.0502 suggest that these two absorptions are due to antisymmetric and symmetric OFeO stretching vibrations. The isotopic spectral features in the mixed $^{16}O_2$ + $^{18}O_2$ and $^{16}O_2$ + $^{16}O^{18}O$ + $^{18}O_2$ experiments (Figure 3) indicate that only one OFeO moiety is involved in these modes. Accordingly, the 1204.5, 975.3, and 871.6 cm^{-1} absorptions are assigned to a (η^1-O$_2$)FeO$_2$ complex, in which an O_2 molecule is end-on bound to the OFeO moiety.

To validate the experimental assignment and to obtain insight into the structure and bonding of the (η^1-O$_2$)FeO$_2$ complex, we performed density functional theory calculations. Two limiting high-symmetry geometries were considered: a planar C_s form in which all five atoms lie in the same plane, and a nonplanar

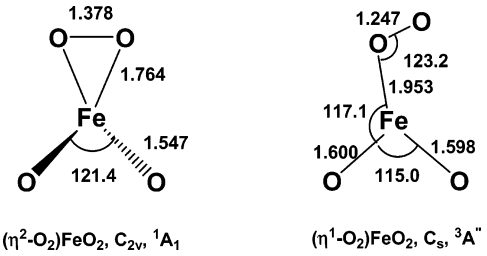

Figure 5. Optimized (DFT/B3LYP) structures of the products (bond lengths in angstrom and bond angles in degree).

C_s form in which the FeOO plane is perpendicular to the OFeO plane. We have carried out geometry optimization in the singlet, triplet, and quintet spin states. For the nonplanar structure, a $^5A'$ state was predicted to be most stable, with a $^3A''$ state lying 4.3 kcal/mol higher in energy than the $^5A'$ state at the B3LYP level of theory. Geometry optimization on the singlet spin state with end-on bonded O_2 converged to the side-on bonded structure. For the planar structure, a $^3A''$ state was predicted to be most stable, followed by a $^3A'$ state, which lies 12.6 kcal/mol higher in energy above the $^3A''$ state. The planar $^3A''$ state structure was computed to be about 1.4 kcal/mol more stable than the $^5A'$ nonplanar isomer at the DFT/B3LYP level of theory. At the CCSD(T)//B3LYP level of theory, the planar structure is also more stable than the nonplanar structure but with a larger energy gap of 6.1 kcal/mol. The planar structure of (η^1-O$_2$)FeO$_2$ is similar to that of the recently reported (η^1-O$_2$)GaO$_2$ complex.[26] As shown in Figure 5, the O−O bond length of the planar $^3A''$ state (η^1-O$_2$)FeO$_2$ complex was calculated to be 1.247 Å with an O−O stretching frequency of 1310.6 cm^{-1}, 8.8% higher than the observed value. The end-on bonded O_2 fragment is due to a superoxide ligand;[27,28] therefore, the (η^1-O$_2$)FeO$_2$ complex can be regarded as an end-on bonded superoxo iron dioxide complex, [(FeO$_2$)$^+$(O$_2^-$)], that is, a FeO_2^+ cation coordinated by one O_2^- anion. The antisymmetric and symmetric OFeO stretching modes were calculated at 956.7 and 921.0 cm^{-1}, respectively, which are about 1.9% lower and 5.7% higher than the experimental values. Although the calculated frequencies (Table 2) do not match the experimental frequencies as well as we would like, the predicted isotopic frequency ratios are in quite good agreement with the experimental values, as listed in Table 3. Vibrational frequency computations for such triplet state iron species are not yet an exact science. The same type of discrepancy has been found for the recently reported (η^1-O$_2$)MO$_2$ complexes (M = Ga, In, Co) as well.[26,29] Taking the (η^1-O$_2$)GaO$_2$ complex as an example, the symmetric and antisymmetric OGaO stretching modes were predicted at 662.7 and 732.3 cm^{-1}, about 7.5% lower and 28.8% higher than the observed frequencies.[26]

(η^2-O$_2$)FeO$_2$. The 955.8 cm^{-1} absorption corresponds to the absorption reported at 956 cm^{-1} that was previously assigned to the O−O stretching (ν_1) mode of cyclic Fe(O$_2$).[3−6] The observed isotopic shift in the present experiments is the same as that reported previously. The cyclic Fe(O$_2$) assignment is questionable since gas phase investigations have indicated that ground state iron atoms are unreactive with dioxygen,[7,8] but the previous matrix isolation investigations showed that the 956 cm^{-1} absorption increased on annealing.[3−6] The present experiments provide strong evidence that the assignment to isolated cyclic Fe(O$_2$) is incorrect and that the 955.8 cm^{-1} absorption should be reassigned to the symmetric OFeO stretching mode of the (η^2-O$_2$)FeO$_2$ complex. As shown in Figure 1, the 955.8 cm^{-1} absorption appeared on annealing at the expense of the inserted FeO_2 molecule absorptions. When the sample was annealed directly after deposition without

TABLE 1: Product Absorptions (cm^{-1}) from the Reactions of Laser-Evaporated Iron Atoms with Dioxygen in Solid Argon

$^{16}O_2$	$^{18}O_2$	$^{16}O_2 + {}^{18}O_2$	$^{16}O_2 + {}^{16}O^{18}O + {}^{18}O_2$	assignment
1094.7	1047.0	1094.7, 1084.8, 1058.5, 1047.0	1094.7, 1089.6, 1084.8, 1058.5, 1052.7, 1047.0	(η^2-O_2)FeO_2 combination mode
968.8	931.2	968.8, 955.6, 931.2, 919.3	968.8, 956.3, 954.1, 931.1, 919.3, 907.8	(η^2-O_2)FeO_2 (FeO_2 asym. str.)
955.8	906.6	906.6, 898.6	906.6, 898.5, 886.3	(η^2-O_2)FeO_2 (FeO_2 sym. str.)
558.1	532.3			(η^2-O_2)FeO_2 (Fe−O_2 asym. str.)
548.3	524.8			(η^2-O_2)FeO_2 (Fe−O_2 sym. str.)
1204.5	1137.1	1204.5, 1203.3, 1138.3, 1137.1	1204.1, 1172.8, 1170.3, 1137.8	(η^1-O_2)FeO_2 (OO str.)
975.3	938.1	975.3, 938.1	975.3, 959.9, 938.1	(η^1-O_2)FeO_2 (FeO_2 asym. str.)
871.6	829.9	871.6, 870.5, 830.9, 829.9	871.2, 847.3, 830.3	(η^1-O_2)FeO_2 (FeO_2 sym. str.)

TABLE 2: DFT/B3LYP Calculated Total Energies (in Hartree, after Zero-Point Energy Corrections), Frequencies (cm^{-1}), and Intensities (km/mol) of the Products

molecule	energy[a]	frequency (intensity)
(η^2-O_2)FeO_2	−1564.494974	1069.4 (199), 1034.0 (190), 1023.5 (0), 616.4 (1),
($^1A_1$, C_{2v})	(−1562.744449)	602.2 (8), 336.4 (4), 325.0 (0), 270.8 (1), 268.9 (6)
(η^1-O_2)FeO_2	−1564.499732	1310.6 (677), 956.7 (109), 921.0 (207), 350.1 (21),
($^3A''$, C_s)	(−1562.713975)	304.5 (2), 195.0 (46), 113.2 (7), 100.4 (23), 74.9 (24)

[a] The values in parentheses are single-point energies calculated at the CCSD(T)//B3LYP level of theory.

TABLE 3: Comparison between the Observed and Calculated Vibrational Frequencies (cm^{-1}) and Isotopic Frequency Ratios of the Product Molecules

		freq		$^{16}O/^{18}O$	
molecule	mode	calcd	obsd	calcd	obsd
(η^2-O_2)FeO_2	FeO_2 asym. str. (b_1)	1069.4	968.8	1.0406	1.0404
	FeO_2 sym. str. (a_1)	1034.0	955.8	1.0503	1.0543
	Fe−O_2 sym. str. (a_1)	616.4	548.3	1.0440	1.0448
	Fe−O_2 asym. str. (b_2)	602.2	558.1	1.0495	1.0485
(η^1-O_2)FeO_2	OO str. (a′)	1310.6	1204.5	1.0609	1.0593
	FeO_2 asym. str. (a′)	956.7	975.3	1.0416	1.0397
	FeO_2 sym. str. (a′)	921.0	871.6	1.0490	1.0502

presentation of the FeO_2 absorptions, the 955.8 cm^{-1} absorption was not observed. This new information suggests that the species responsible for the 955.8 cm^{-1} absorption is a reaction product of FeO_2 and not Fe atoms. Along with the 955.8 cm^{-1} absorption, other absorptions at 1094.7, 968.8, 558.1, and 548.3 cm^{-1} showed identical behavior following irradiation and annealing, implying that these absorptions are due to different vibrational modes of the same species. We checked the spectra reported in the literature[3,6] and found that an absorption around 969 cm^{-1} was present in the spectra, which showed the same behavior as the 956 cm^{-1} absorption as well. The present experiments also showed that the 955.8 cm^{-1} and related absorptions are photoreversible with the (η^1-O_2)FeO_2 absorptions, which suggests that the species responsible for these absorptions is a structural isomer of (η^1-O_2)FeO_2. These absorptions are assigned to the (η^2-O_2)FeO_2 complex. The 968.8 cm^{-1} absorption was already attributed to the antisymmetric OFeO stretching mode of (η^2-O_2)FeO_2 due to its isotopic ratio of 1.0404 in the previous report.[6] The 955.8 cm^{-1} absorption shifted to 906.6 cm^{-1} with an $^{16}O/^{18}O$ isotopic frequency ratio of 1.0543, which is appropriate for a symmetric OFeO stretching mode. As shown in Figure 4, the spectral features in the experiments with mixed isotopic samples are complicated due to mode mixing. Besides the absorptions observed in the $^{16}O_2$/Ar and $^{18}O_2$/Ar experiments, two supplementary absorptions at 919.3 and 898.6 cm^{-1} were observed in the spectrum with an equal molar mixture of $^{16}O_2$ and $^{18}O_2$ (Figure 4, trace c). The 955.8 cm^{-1} absorption is broadened, and the band center shifted to 955.6 cm^{-1} with its relative intensity greater than what would be expected, implying that an additional intermediate absorption is located in this frequency. The spectrum with the mixed $^{16}O_2 + {}^{16}O^{18}O + {}^{18}O_2$ (1:2:1) sample (Figure 4, trace d) is even more complicated. As shown in Figure 4 trace d, seven intermediate absorptions located at 956.3, 954.1, 931.1, 919.3, 907.8, 898.5, and 886.3 cm^{-1} were resolved. The O−O stretching mode of the (η^2-O_2)FeO_2 complex was not observed, but two Fe−O_2 vibrations were observed at 558.1 and 548.3 cm^{-1}. The weak absorption at 1094.7 cm^{-1} corresponds to the absorption reported at 1095.4 cm^{-1}, which was previously assigned to the O−O stretching mode of the (η^2-O_2)FeO_2 complex.[6] This absorption shifted to 1047.0 cm^{-1} with the $^{18}O_2$/Ar sample. The resulting $^{16}O/^{18}O$ isotopic frequency ratio of 1.0456 is too low for an O−O stretching mode. The 1094.7 cm^{-1} absorption presents a quartet structure composed of the two absorptions observed in the $^{16}O_2$/Ar and $^{18}O_2$/Ar experiments and of two additional absorptions at 1084.8 and 1058.5 cm^{-1} in the experiment with an equal molar mixture of $^{16}O_2$ and $^{18}O_2$. In the experiment with a 1:2:1 mixture of $^{16}O_2/^{16}O^{18}O/^{18}O_2$, a sextet with two additional intermediates at 1089.6 and 1052.7 cm^{-1} was observed. This absorption is most likely due to a combination mode of the Fe−O_2 vibrations observed at 558.1 and 548.3 cm^{-1}. Previous anion photoelectron spectroscopic study on the FeO_4^- anion gave a vibrational frequency of 920 ± 50 cm^{-1} for the ground state of (η^2-O_2)-FeO_2 neutral,[10] which is very close to the observed FeO_2 stretching frequency in solid argon.

The FeO_4 molecule has been the subject of several theoretical calculations.[16−18] Pure DFT calculations found that a tetraoxide structure (T_d symmetry) without O−O bonding is more stable than the (η^2-O_2)FeO_2 structure, which was predicted to have a singlet ground state with a nonplanar C_{2v} symmetry.[16,17] However, ab initio and hybrid DFT calculations revealed that the tetraoxide structure is less stable than the (η^2-O_2)FeO_2 structure.[18] The T_d structure of FeO_4 has only one IR active Fe═O stretching mode, and therefore it does not fit the observed spectrum. We performed theoretical calculations on the (η^2-O_2)FeO_2 structure with C_{2v} symmetry. At the B3LYP/6-311+G(d) level of theory, a $^3A_1$ state was predicted to be slightly (0.1 kcal/mol) more stable than the $^1A_1$ state, which was previously reported to be the ground state of (η^2-O_2)FeO_2. However, the singlet state was predicted to be about 17.1 kcal/mol more stable than the triplet state at the CCSD(T)//B3LYP level of theory. As listed in Tables 2 and 3, both the calculated vibrational frequencies and isotopic frequency ratios of the singlet state (η^2-O_2)FeO_2 fit the observed values quite well. Note that the O−O stretching mode of the (η^2-O_2)FeO_2 complex was predicted to absorb at 1023.5 cm^{-1} with very low IR intensity, and hence it could not be observed in the experiments. As shown in Figure 5, the O−O bond length was predicted to be 1.378

TABLE 4: Calculated Vibrational Frequencies (cm^{-1}) and Intensities (km/mol) of Different (η^2-O_2)FeO_2 Isotopomers

molecule	frequency (intensity)		
	FeO_2 asym. str.	FeO_2 sym. str.	OO str.
(η^2-$^{16}O_2$)$Fe^{16}O_2$	1069.4 (199)	1034.0 (190)	1023.5 (0)
(η^2-$^{16}O_2$)$Fe^{18}O_2$	1027.8 (185)	977.2 (40)	1031.2 (146)
(η^2-$^{18}O_2$)$Fe^{16}O_2$	1069.3 (199)	1027.8 (88)	972.4 (90)
(η^2-$^{18}O_2$)$Fe^{18}O_2$	1027.7 (185)	984.5 (161)	966.2 (13)
(η^2-$^{16}O^{18}O$)$Fe^{16}O_2$	1069.3 (199)	1028.4 (107)	1001.2 (77)
(η^2-$^{16}O_2$)$Fe^{16}O^{18}O$	1057.9 (180)	992.5 (55)	1031.1 (145)
(η^2-$^{16}O^{18}O$)$Fe^{16}O^{18}O$	1057.9 (179)	989.7 (20)	1005.9 (175)
(η^2-$^{16}O^{18}O$)$Fe^{18}O_2$	1027.8 (185)	975.5 (20)	1004.7 (160)
(η^2-$^{18}O_2$)$Fe^{16}O^{18}O$	1057.8 (178)	995.6 (130)	970.6 (59)

Å, which falls into the range of peroxide bond lengths;[27] therefore, the (η^2-O_2)FeO_2 complex can be regarded as [$(FeO_2)^{2+}(O_2^{2-})$], a side-on bonded peroxo iron dioxide complex. The complex was predicted to have a smaller OFeO bond angle (121.4°) than those of the iron dioxide complexes with acetylene (130.6°) and ethylene (137.4°),[30] which is consistent with the relatively larger isotopic frequency ratio of the antisymmtric OFeO stretching mode in the (η^2-O_2)FeO_2 complex. The mixed isotopic spectral features are complicated. As listed in Table 4, the O−O stretching mode of (η^2-$^{16}O_2$)$Fe^{16}O_2$ has zero IR intensity, but this mode of partially oxygen-18 substituted isotopomers exhibits quite strong IR intensities due to mode coupling. The calculated isotopic spectral features are in reasonable agreement with the experimental observations.

The end-on and side-on coordination of dioxygen has been observed in many transition metal oxide clusters. The structures of FeO_4 complexes are very similar to those CrO_5 and WO_5.[31,32] The CrO_5 species was characterized to have a (η^1-O_2)CrO_3 structure with an O−O bond length of 1.22 Å.[31] The WO_5 molecule was predicted to be a side-on bonded superoxo tungsten trioxide with an O−O bond length of 1.312 Å.[32]

Reaction Mechanism. The spectra in Figure 1 recorded after laser ablation and co-deposition of iron and dioxygen using low laser energy clearly show that no metal based absorptions were observed after sample deposition. The O_4^- absorption arises from the capture of laser ablated electrons as described previously.[24] The inserted FeO_2 absorptions were produced here only under broad band UV−visible irradiation, which indicates that the formation of inserted FeO_2 from atomic iron and O_2 requires activation energy, as proposed previously.[6] Previous investigation indicated that the interaction between the ground state iron atom and dioxygen is repulsive.[8] Although it is at first surprising that the 946 cm^{-1} absorption ultimately assigned as the inserted FeO_2 molecule[6] was first observed from the reaction of "thermal" iron atoms,[2] it must be noted that the use of an electron beam furnace for 1950 K atoms can provide adequate radiation to activate the reaction. We found that UV and visible light irradiation are able to initiate the insertion reaction to form FeO_2. The UV−visible absorption spectra and laser-induced fluorescence spectra of iron atoms isolated in solid argon have been measured.[33] There are numerous transitions in the UV and visible spectral regions with some excited states having quite long lifetime, which may responsible for the insertion reaction.[34] It is significant that no absorptions were observed in Figure 1 spectra that can be assigned to simple isolated cyclic Fe(O_2) and bent FeOO complexes. These experimental observations are consistent with previous gas phase investigations, which found that the ground state iron atoms are unreactive toward dioxygen,[7,8] and only the inserted FeO_2 structure was observed from anion photoelectron spectra.[9,10] When the deposited samples were first subjected to UV−visible irradiation and then annealed to 25 K, the (η^1-O_2)FeO_2 and (η^2-O_2)FeO_2 complexes were formed. As shown in Figure 1, only the FeO_2 absorptions were observed after UV−visible light irradiation of the as-deposited samples, which decreased upon subsequent sample annealing. These observations indicate that the (η^1-O_2)FeO_2 and (η^2-O_2)FeO_2 complexes are formed via the reactions of FeO_2 with O_2 upon sample annealing, reactions 1 and 2. The complex absorptions increased on sample annealing, indicating that both reactions require negligible activation energy. At the CCSD(T)//B3LYP level of theory, reactions 1 and 2 were predicted to be exothermic by 25.9 and 6.8 kcal/mol, respectively.

$$FeO_2\,(^3B_1) + O_2\,(^3\Sigma_g^-) \rightarrow (\eta^2\text{-}O_2)FeO_2\,(^1A_1) \qquad \Delta E = -25.9 \text{ kcal/mol} \quad (1)$$

$$FeO_2\,(^3B_1) + O_2\,(^3\Sigma_g^-) \rightarrow (\eta^1\text{-}O_2)FeO_2\,(^3A'') \qquad \Delta E = -6.8 \text{ kcal/mol} \quad (2)$$

Our experiments clearly show that the end-on and side-on bonded iron dioxide−dioxygen complexes are photoreversible: near-infrared light ($\lambda > 850$ nm) irradiation induces the conversion of the side-on bonded (η^2-O_2)FeO_2 complex to the end-on bonded (η^1-O_2)FeO_2 isomer and vice versa with red light irradiation ($\lambda > 600$ nm). The end-on bonded complex has a triplet ground state, while the side-on bonded structure has a singlet ground state. Therefore, the isomerization process involves spin crossing.

Both the end-on and side-on bonded cobalt dioxide−dioxygen complexes were observed in a recent matrix isolation infrared investigation on the reaction of CoO_2 and molecular O_2 in solid rare gas matrixes.[26] The results demonstrate that the end-on bonded (η^1-O_2)CoO_2 complex was formed first, followed by relaxation to the side-on bonded structure. The end-on bonded structure was characterized to be an excited state of CoO_4 with a lifetime around 23 ± 2 min in argon. It is difficult to judge which structure is formed first in the case of FeO_4, since both the end-on and side-on bonded complexes were observed on annealing. We assume that the end-on bonded structure is formed first, which can be isomerized to the side-on bonded isomer during annealing. The bent FeO_2 molecule was determined to have a triplet ground state, and the O_2 molecule also has a $^3\Sigma$ ground state.[6,13,14] It seems reasonable that the reaction forms the triplet end-on bonded FeO_4 first rather than the singlet side-on bonded isomer. In contrast to the end-on bonded (η^1-O_2)CoO_2 complex which was characterized as an excited state of CoO_4,[26] the end-on bonded (η^1-O_2)FeO_2 complex is a stable isomer of FeO_4 and should not be regarded as an excited state of FeO_4. Although the (η^1-O_2)FeO_2 absorptions decreased with increasing the scan times due to the red irradiation from the source, the (η^1-O_2)FeO_2 absorptions do not change significantly when the sample was kept in the dark. This also implies that the process from the end-on bonded structure to the side-on bonded isomer requires some activation energy.

Conclusions

The reaction of iron atoms with dioxygen has been reinvestigated using matrix isolation infrared absorption spectroscopy and lower laser energy to minimize photochemistry. It is found that the ground state iron atoms are unreactive with O_2 in solid argon and that inserted FeO_2 molecules were produced only under broad band UV−visible irradiation. Annealing allows the dioxygen molecules to diffuse and react with FeO_2 to form the side-on and end-on bonded dioxygen−iron dioxide complexes, (η^2-O_2)FeO_2 and (η^1-O_2)FeO_2. The side-on bonded structure is

characterized to be a peroxo iron dioxide complex having a singlet ground state with a nonplanar C_{2v} symmetry. The end-on bonded isomer is calculated to be a superoxo iron dioxide complex with a planar $^3A''$ ground state. These two isomers are photoreversible, that is, near-infrared light ($\lambda > 850$ nm) induces the conversion of the side-on bonded (η^2-O_2)FeO_2 complex to the end-on bonded (η^1-O_2)FeO_2 isomer, and the reverse with red light irradiation ($\lambda > 600$ nm).

Acknowledgment. This work is supported by National Basic Research Program of China (2007CB815203), National Natural Science Foundation of China (20433080), and the Committee of Science and Technology of Shanghai (04JC14016).

References and Notes

(1) See for example: (a) Momenteau, M.; Reed, C. A. *Chem. Rev.* **1994**, *94*, 659. (b) Kovaleva, E. G.; Neibergall, M. B.; Chakrabarty, S.; Lipscomb, J. D. *Acc. Chem. Res.* **2007**, *40*, 475. (c) Girerd, J. J.; Banse, F.; Simaan, A. J. *Struct. Bonding* **2000**, *97*, 145.

(2) Abramowitz, S.; Acquista, N.; Levin, I. W. *Chem. Phys. Lett.* **1977**, *50*, 423.

(3) Chang, S.; Blyholder, G.; Fernandez, J. *Inorg. Chem.* **1981**, *20*, 2813.

(4) Fanfarillo, M.; Downs, A. J.; Green, T. M.; Almond, M. J. *Inorg. Chem.* **1992**, *31*, 2973.

(5) Yamada, Y.; Sumino, H.; Okamura, Y.; Shimasaki, H.; Tominaga, T. *Appl. Radiat. Isot.* **2000**, *52*, 157.

(6) (a) Andrews, L.; Chertihin, G. V.; Ricca, A.; Bauschlicher, C. W., Jr. *J. Am. Chem. Soc.* **1996**, *118*, 467. (b) Chertihin, G. V.; Saffel, W.; Yustein, J. T.; Andrews, L.; Neurock, M.; Ricca, A.; Bauschlicher, C. W., Jr. *J. Phys. Chem.* **1996**, *100*, 5261.

(7) Whetten, R. L.; Cox, D. M.; Trevor, D. J.; Kaldor, A. *J. Phys. Chem.* **1985**, *89*, 566.

(8) Mitchell, S. A.; Hackett, P. A. *J. Chem. Phys.* **1990**, *93*, 7822.

(9) Fan, J.; Wang, L. S. *J. Chem. Phys.* **1995**, *102*, 8714.

(10) (a) Wu, H. B.; Desai, S. R.; Wang, L. S. *J. Am. Chem. Soc.* **1996**, *118*, 5296. (b) Wu, H. B.; Desai, S. R.; Wang, L. S. *J. Am. Chem. Soc.* **1996**, *118*, 7434.

(11) Schröder, D.; Fiedler, A.; Schwarz, J.; Schwarz, H. *Inorg. Chem.* **1994**, *33*, 5094.

(12) Uzunova, E. L.; Nikolov, G. St.; Mikosch, H. *ChemPhysChem* **2004**, *5*, 192.

(13) Gutsev, G. L.; Rao, B. K.; Jena, P. *J. Phys. Chem. A* **2000**, *104*, 11961.

(14) García-Sosa, A. T.; Castro, M. *Int. J. Quantum Chem.* **2000**, *80*, 307.

(15) Cao, Z.; Duran, M.; Solà, M. *Chem. Phys. Lett.* **1997**, *274*, 411.

(16) Gutsev, G. L.; Khanna, S. N.; Rao, B. K.; Jena, P. *J. Phys. Chem. A* **1999**, *103*, 5812.

(17) Atanasov, M. *Inorg. Chem.* **1999**, *38*, 4942.

(18) Cao, Z.; Wu, W.; Zhang, Q. *J. Mol. Struct. (Theochem)* **1999**, *489*, 165.

(19) (a) Zhou, M. F.; Andrews, L.; Bauschlicher, C. W., Jr. *Chem. Rev.* **2001**, *101*, 1931. (b) Wang, G. J.; Gong, Y.; Chen, M. H.; Zhou, M. F. *J. Am. Chem. Soc.* **2006**, *128*, 5974. (c) Zhou, M. F.; Tsumori, N.; Xu, Q.; Kushto, G. P.; Andrews, L. *J. Am. Chem. Soc.* **2003**, *125*, 11371.

(20) *Gaussian 03*, Revision B.05; Frisch, M. J.; Trucks, G. W.; Schlegel, H. B.; Scuseria, G. E.; Robb, M. A.; Cheeseman, J. R.; Montgomery, J. A., Jr.; Vreven, T.; Kudin, K. N.; Burant, J. C.; Millam, J. M.; Iyengar, S. S.; Tomasi, J.; Barone, V.; Mennucci, B.; Cossi, M.; Scalmani, G.; Rega, N.; Petersson, G. A.; Nakatsuji, H.; Hada, M.; Ehara, M.; Toyota, K.; Fukuda, R.; Hasegawa, J.; Ishida, M.; Nakajima, T.; Honda, Y.; Kitao, O.; Nakai, H.; Klene, M.; Li, X.; Knox, J. E.; Hratchian, H. P.; Cross, J. B.; Adamo, C.; Jaramillo, J.; Gomperts, R.; Stratmann, R. E.; Yazyev, O.; Austin, A. J.; Cammi, R.; Pomelli, C.; Ochterski, J. W.; Ayala, P. Y.; Morokuma, K.; Voth, G. A.; Salvador, P.; Dannenberg, J. J.; Zakrzewski, V. G.; Dapprich, S.; Daniels, A. D.; Strain, M. C.; Farkas, O.; Malick, D. K.; Rabuck, A. D.; Raghavachari, K.; Foresman, J. B.; Ortiz, J. V.; Cui, Q.; Baboul, A. G.; Clifford, S.; Cioslowski, J.; Stefanov, B. B.; Liu, G.; Liashenko, A.; Piskorz, P.; Komaromi, I.; Martin, R. L.; Fox, D. J.; Keith, T.; Al-Laham, M. A.; Peng, C. Y.; Nanayakkara, A.; Challacombe, M.; Gill, P. M. W.; Johnson, B.; Chen, W.; Wong, M. W.; Gonzalez, C.; Pople, J. A. Gaussian, Inc.: Pittsburgh, PA, 2003.

(21) Becke, A. D. *J. Chem. Phys.* **1993**, *98*, 5648.

(22) Lee, C.; Yang, W.; Parr, R. G. *Phys. Rev. B* **1988**, *37*, 785.

(23) (a) McLean, A. D.; Chandler, G. S. *J. Chem. Phys.* **1980**, *72*, 5639. (b) Krishnan, R.; Binkley, J. S.; Seeger, R.; Pople, J. A. *J. Chem. Phys.* **1980**, *72*, 650.

(24) Chertihin, G. V.; Andrews, L. *J. Chem. Phys.* **1998**, *108*, 6404.

(25) Zhao, Y. Y.; Gong, Y.; Zhou, M. F. *J. Phys. Chem. A* **2006**, *110*, 10777.

(26) Gaertner, B.; Köhn, A.; Himmel, H. J. *Eur. J. Inorg. Chem.* **2006**, 1496.

(27) (a) Cramer, C. J.; Tolman, W. B.; Theopold, K. H.; Rheingold, A. L. *Proc. Natl. Acad. Sci. U.S.A.* **2003**, *100*, 3635. (b) Hill, H. A. O.; Tew, D. G. *Comprehensive Coordination Chemistry*; Wilkinson, G., Gillard, R. D., McCleverty, J. A., Eds.; Pergamon: Oxford, 1987; Vol. 2, p 315. (c) Vaska, L. *Acc. Chem. Res.* **1976**, *9*, 175. (d) Valentine, J. S. *Chem. Rev.* **1973**, *73*, 235.

(28) (a) Gong, Y.; Zhou, M. F.; Tian, S. X.; Yang, J. L. *J. Phys. Chem. A* **2007**, *111*, 6127. (b) Gong, Y.; Zhou, M. F. *J. Phys. Chem. A* **2007**, *111*, 8973.

(29) Danset, D.; Alikhani, M. E.; Manceron, L. *J. Phys. Chem. A* **2005**, *109*, 105.

(30) (a) Zhou, M. F.; Dong, J.; Miao, L. *J. Phys. Chem. A* **2004**, *108*, 2431. (b) Chen, M. H.; Huang, Z. G.; Zhou, M. F. *Chem. Phys. Lett.* **2004**, *384*, 165.

(31) Gutsev, G. L.; Jena, P.; Zhai, H. J.; Wang, L. S. *J. Chem. Phys.* **2001**, *115*, 7935.

(32) Zhai, H. J.; Kiran, B.; Cui, L. F.; Li, X.; Dixon, D. A.; Wang, L. S. *J. Am. Chem. Soc.* **2004**, *126*, 16134.

(33) (a) Mann, D. M.; Broida, H. P. *J. Chem. Phys.* **1971**, *55*, 84. (b) Carstens, D. H. W.; Kozlowski, J. F.; Gruen, D. M. *High. Temp. Sci.* **1972**, *4*, 301. (c) McKenzie, M. T., Jr.; Epting, M. A.; Nixon, E. R. *J. Chem. Phys.* **1982**, *77*, 735.

(34) Celluccit, T. A.; Nixon, E. R. *J. Phys. Chem.* **1985,** *89*, 1991.